Bioprinting of Cartilaginous Auricular Constructs Utilizing an Enzymatically Crosslinkable Bioink

Author(s):
Fisch, Philipp; Broguiere, Nicolas; Finkielsztein, Sergio; Linder, Thomas; Zenobi-Wong, Marcy

Publication date:
2021-04

Permanent link:
https://doi.org/10.3929/ethz-b-000473435

Originally published in:
Advanced Functional Materials 31(16), https://doi.org/10.1002/adfm.202008261

Funding acknowledgement:
173868 - Sinergia Project: A Tissue, Cell and Molecular Approach to Understanding and Treating Microtia (SNF)

Supporting Information

Bioprinting of Cartilaginous Auricular Constructs Utilizing an Enzymatically Crosslinkable Bioink

*Philipp Fisch, Nicolas Broguiere, Sergio Finkielsztein, Thomas Linder, Marcy Zenobi-Wong**

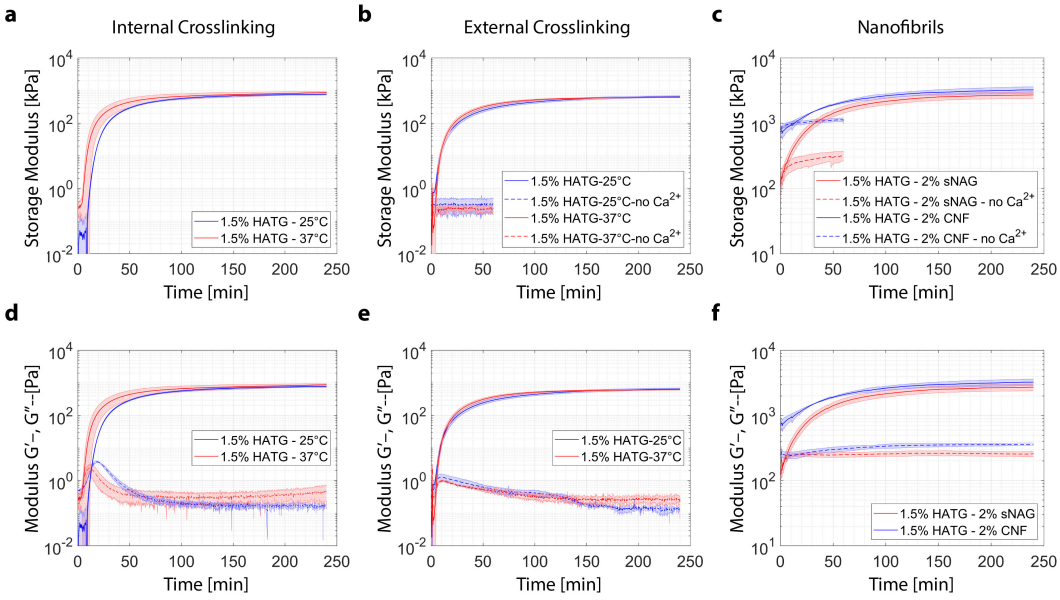

Figure S1. CTEC mechanism compared to conventional crosslinking of HA-TG. a) Traditional method of crosslinking HA-TG with Ca^{2+} present in the polymer solution compared at 25 °C and 37 °C. Addition of FXIII and thrombin therefore triggers crosslinking immediately. b) Crosslinking of HA-TG by diffusion of calcium ions into the sample compared at 25 °C and 37 °C with and without the external addition of 10 µl of 1 M $CaCl_2$. c) Similar to B, HA-TG combined with Nanofibrils was crosslinked by diffusion of calcium ions into the sample at 25 °C and 37 °C. Nanofibrils were added to HA-TG to test whether they would hinder the crosslinking process. In the absence of calcium ions an initial increase in storage modulus was observed likely due to alignment of nanofibrils. d–f) Same plots as in A–C with the additional information of the loss modulus but without uncrosslinked samples. n = 3.

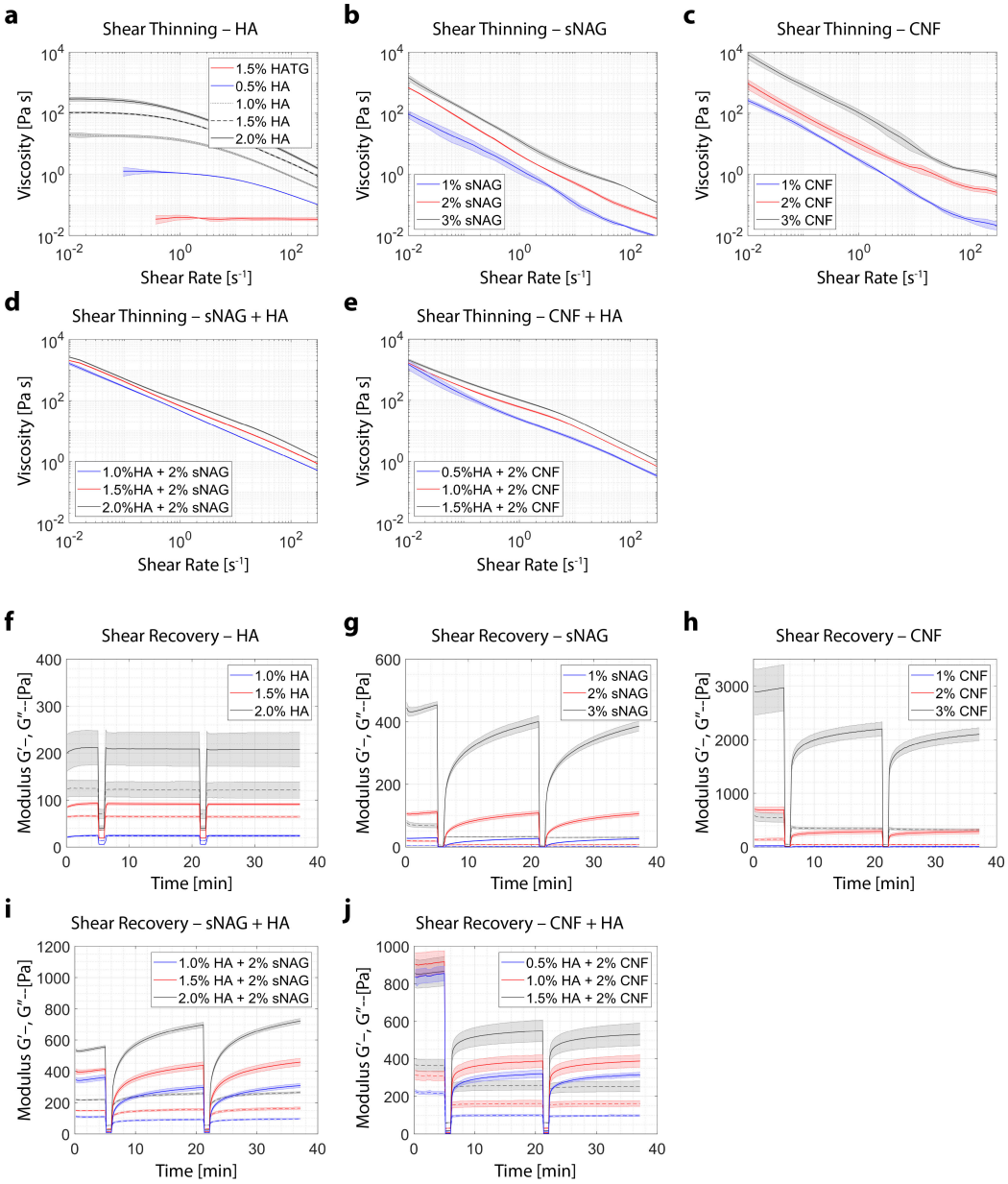

Figure S2. Shear thinning and shear recovery of bioink components. a–e) Shear thinning behavior of the different materials, concentrations and material combinations. HA-TG was neglected for initial testing when mixing nanofibrils with HA due to its low viscosity and timeconsuming synthesis. a) HA at various concentrations and HA-TG at 1.5%. b) sNAG nanofribrils at various concentrations. c) CNF nanofibrils at various concentrations. d**)** sNAG in combination with various concentrations of HA. **e**, CNF in combination with various concentrations of HA. f–j) Shear recovery behavior of different materials, concentrations and material combinations: f) HA at various concentrations. g) sNAG nanofribrils at various concentrations. h) CNF nanofibrils at various concentrations. i) sNAG in combination with various concentrations of HA. j) CNF in combination withvarious concentrations of HA. n = 3.

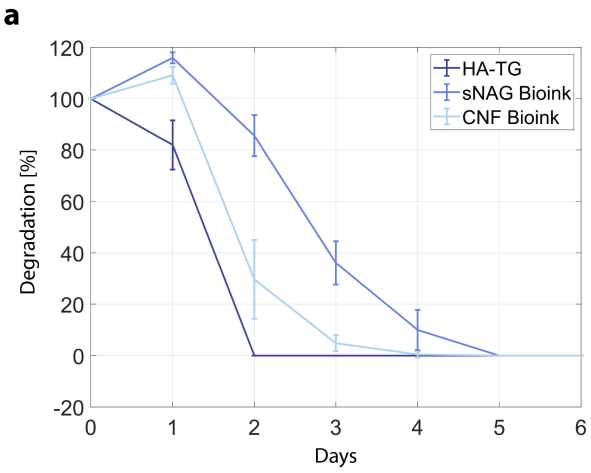

Figure S3. Hyaluronidase degradation study. a) Degradation of HA-TG, sNAG constructs and CNF constructs during incubation with hyaluronidase. n = 6.

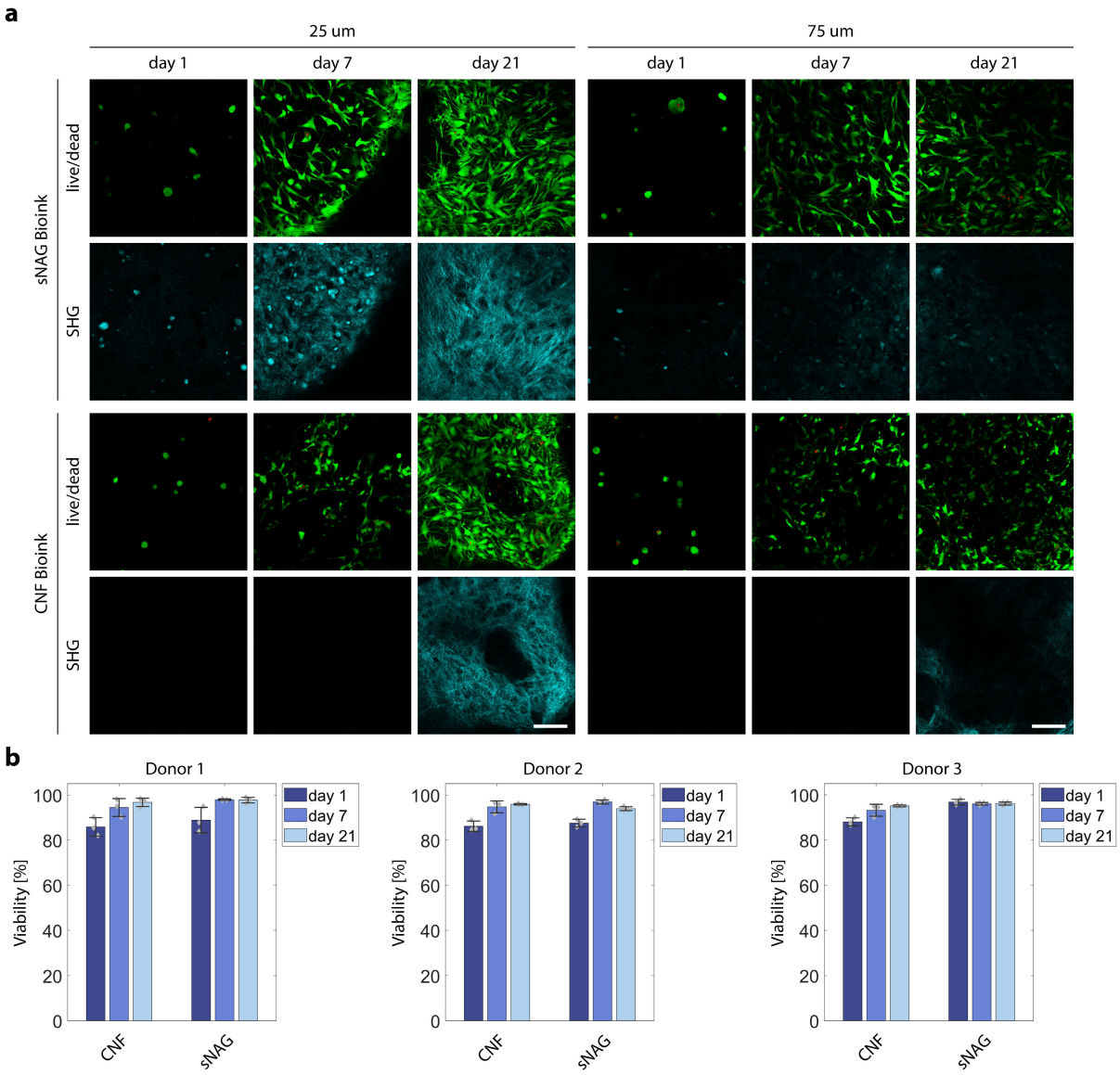

Figure S4. Viability of hAUR at different depths. a) Representative viability and SHG images taken 25 and 75 µm within the sample. Scale bar: 100 µm. b) Viability analysed throughout z-stacks obtained from the surface of the samples up to 100 µm into the samples split according to the different donors of human auricular chondrocytes (donor 1-3). n = 3 per donor.

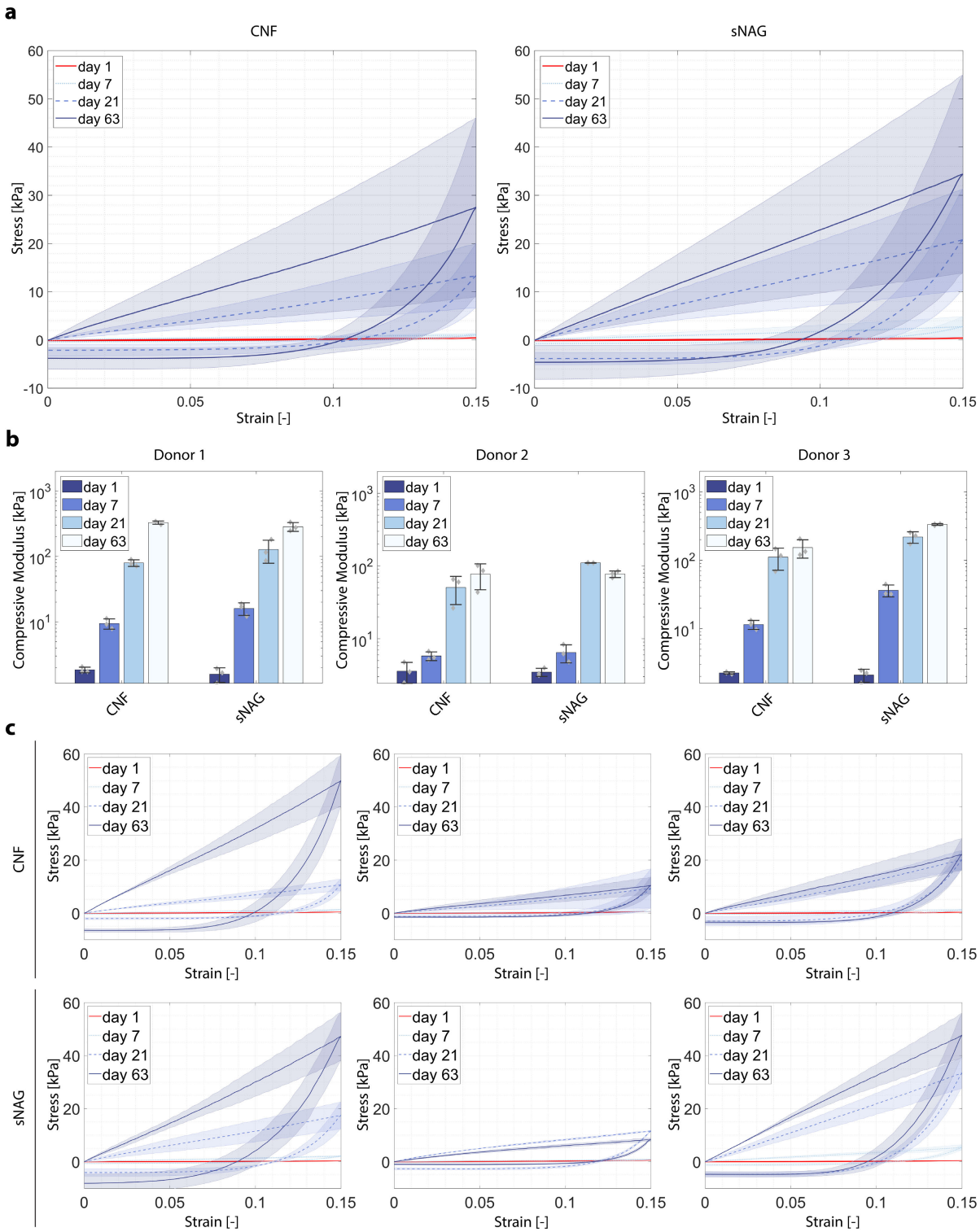

Figure S5. Stress-strain curves and compressive moduli of to the different donors. a) Average stress-strain curves at the different time points for all donors and samples combined. b) Compressive modulus calculated from stress-strain curves at the respective timepoints for the individual donors: donor 1-3. c) Average stress-strain curves at the different time points for the individual donors. n = 3 per donor.

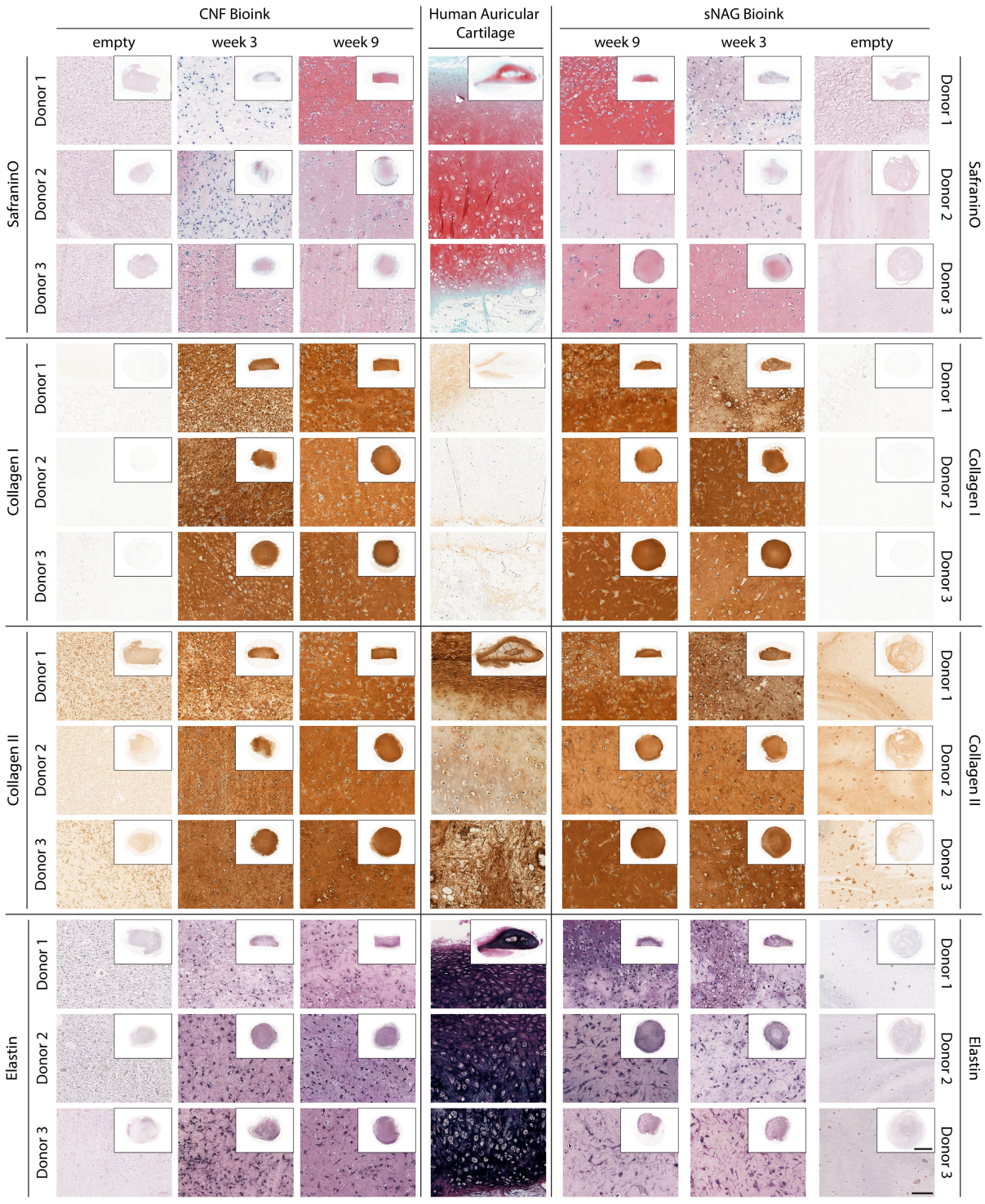

Figure S6. Histological and immunohistological stainings of to the different donors. Histological and immunohistological stainings for GAGs (Safranin O), collagen I, collagen II and elastin compared to human auricular cartilage. Representative images from each donor. Scale bar full sample: 2 mm, Scale bar close up: 100 µm, n = 3 per donor.

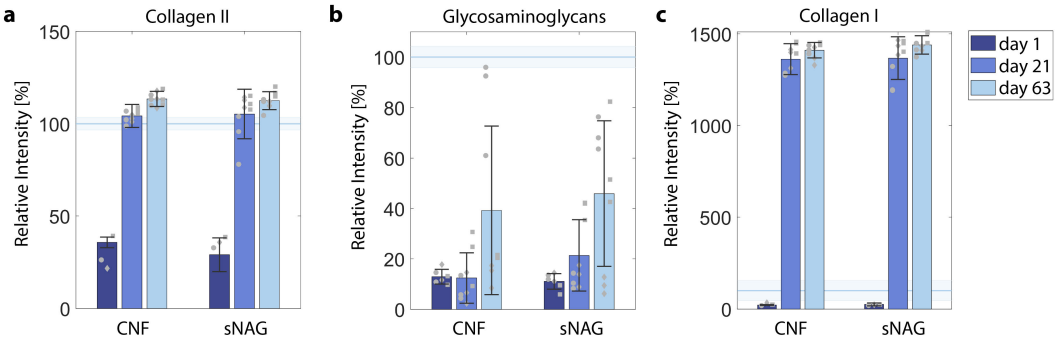

Figure S7. Semi-quantitative analysis of histological and immunohistological stainings. The intensity of histological and immunohistological stainings for a) collagen I, b) GAGs (Safranin O) and c) collagen I were compared to human auricular cartilage (light blue shaded error bar line). • donor 1, ◆ donor 2, ▪ donor 3, n = 9.

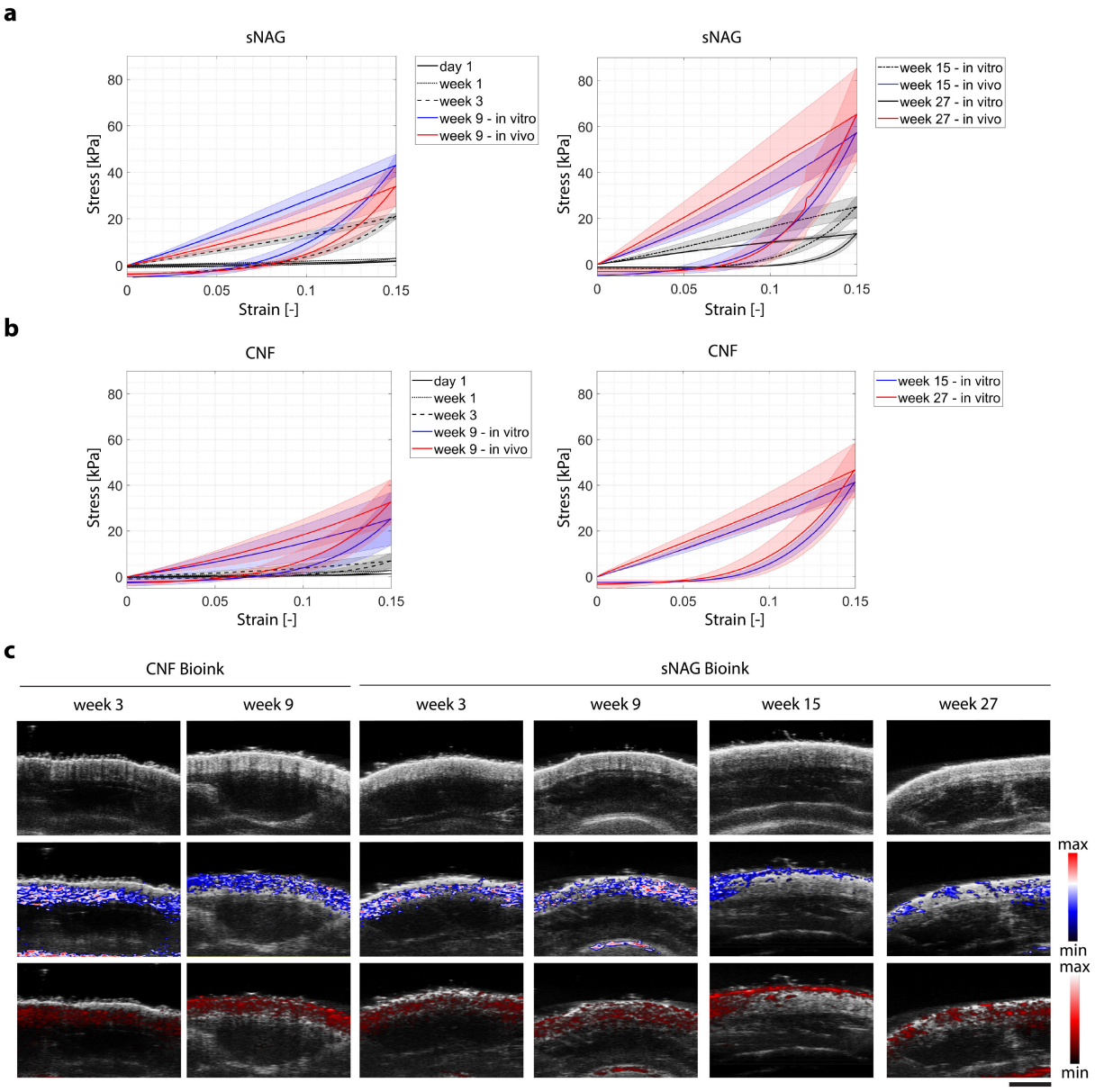

Figure S8. Stress-strain curves and photoacoustic images. a) Stress-strain curves at the respective timepoints averaged for bioprinted sNAG samples and b) stress-strain curves at the respective timepoints averaged for bioprinted CNF samples. n = 3 for *in vitro* and n = 12 for *in vivo*. c) Ultrasound and photoacoustic images obtained after implantation and right before euthanization. Top: Ultrasound, middle: images showing an overlay of ultrasound and oxygen saturation, bottom: images showing an overlay of ultrasound and oxyhemoglobin saturation (λ = 700 nm). Scale bar: 3 mm, n = 4.

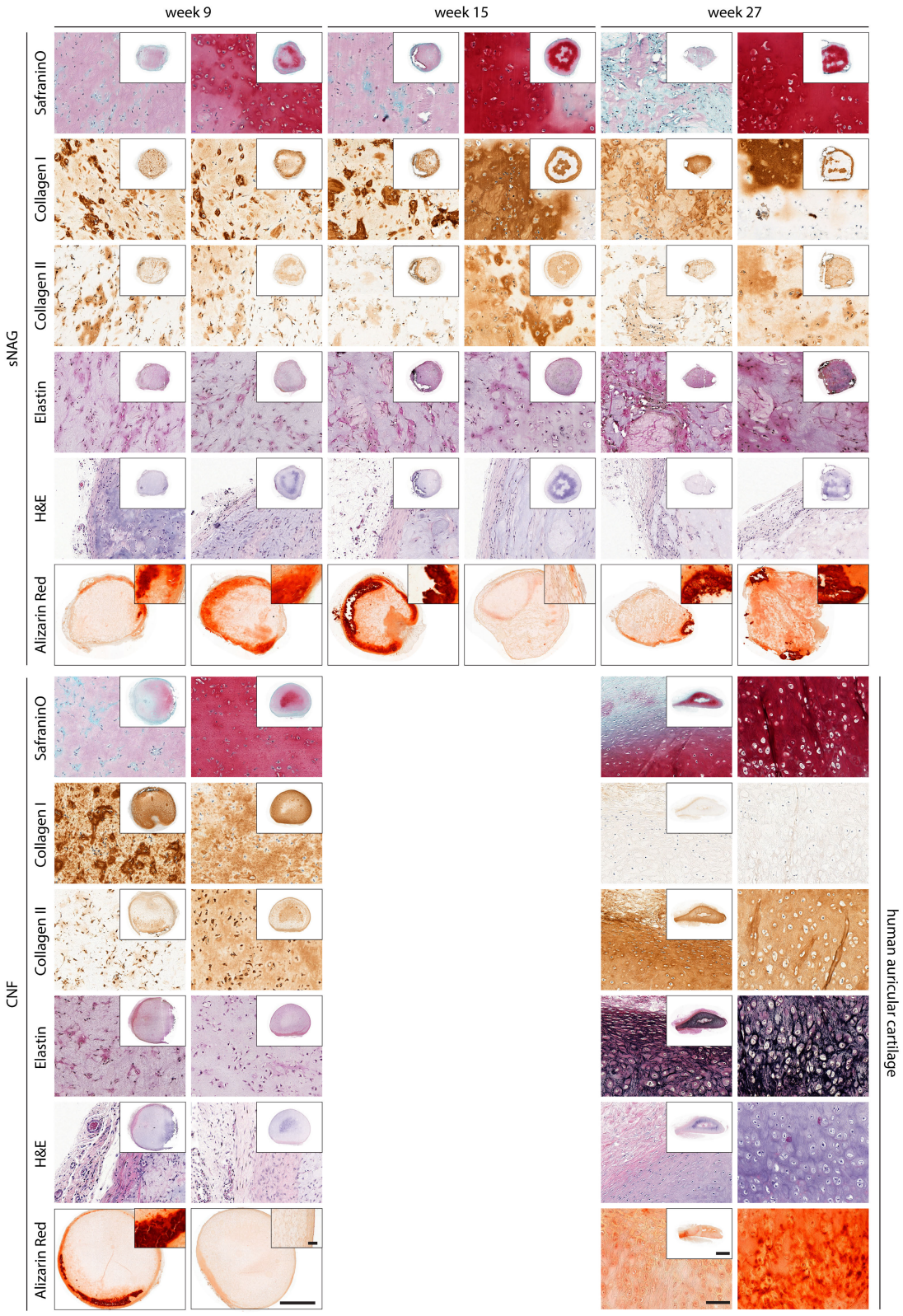

Figure S9. Histological and immunohistological stainings showing best and worst samples at the respective timepoints. Histological and immunohistological stainings for GAGs (Safranin O), collagen I and II, elastin, H&E and alizarin red of *in vivo* constructs after 9, 15 and 27 weeks showing the differences in ECM expression of samples from the same timepoint. Scale bar full sample 2 mm, scale bar close up 100 µm, n = 12.

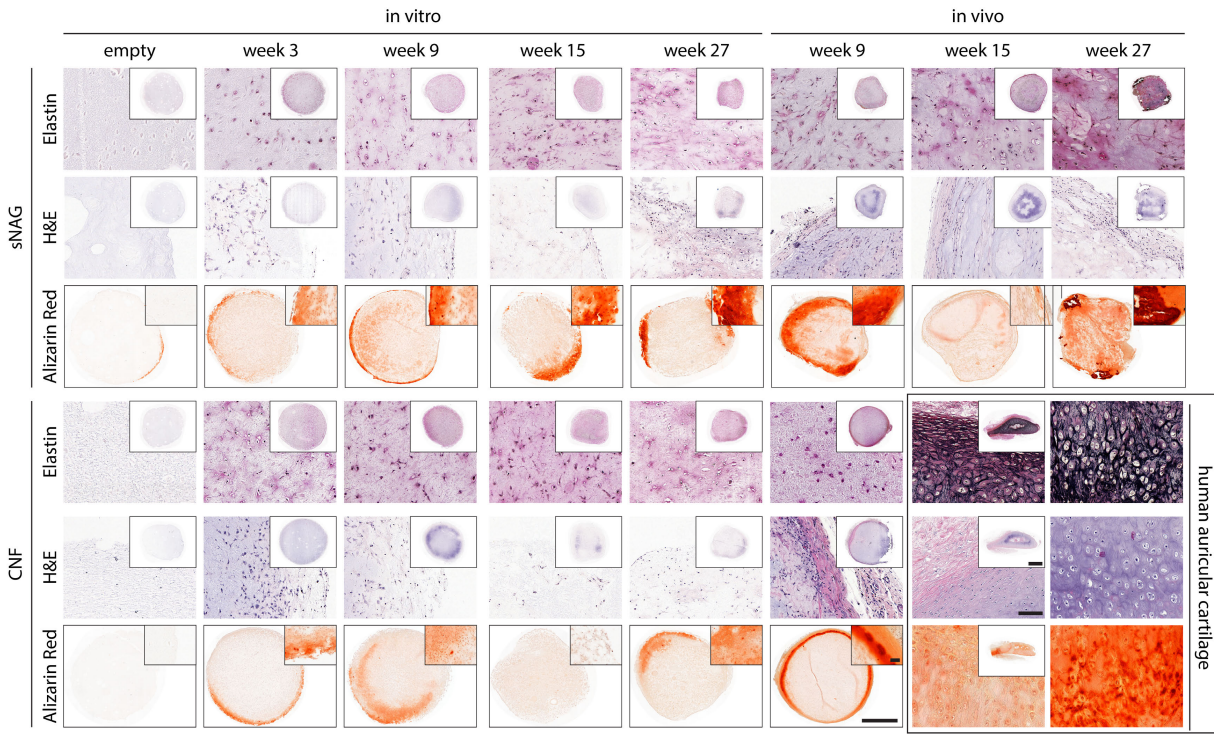

Figure S10. Histological stainings of bioprinted constructs. Histological stainings for elastin, H&E and calcium (Alizarin Red) compared to human auricular cartilage; scale bar full sample 2 mm, scale bar close up 100 µm. Full sample images of samples stained for calcium are depicted larger to show the distribution of calcium throughout the sample. n = 3 for *in vitro* and n = 12 for *in vivo*.

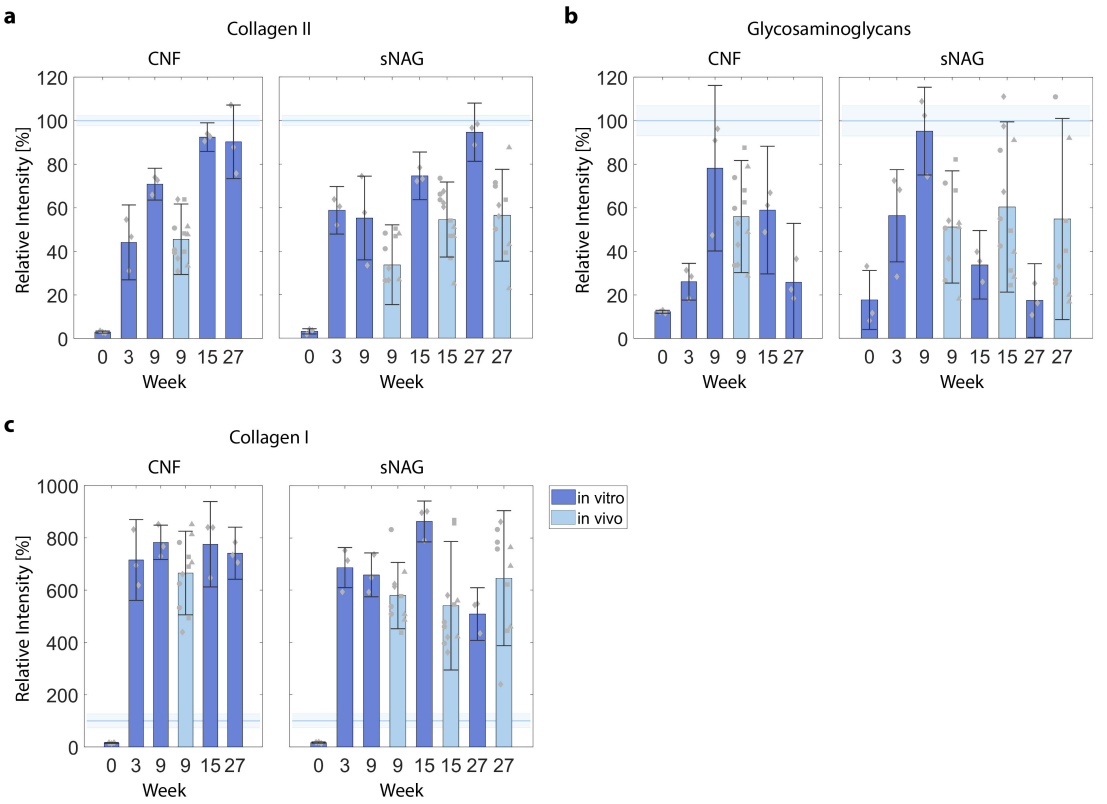

Figure S11. Semi-quantitative analysis of histological and immunohistological stainings. The intensity of histological and immunohistological stainings for a) collagen I, b) GAGs (Safranin O) and c) collagen I were compared to human auricular cartilage (light blue shaded error bar line). • rat 1, ◆ rat 2, ■ rat 3, ▲ rat 4, n = 3 for *in vitro*, n = 10–12 for *in vivo*.

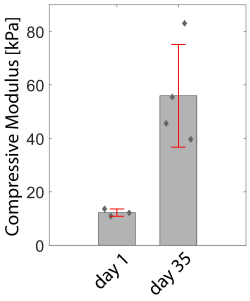

Figure S12. Compressive modulus of bioprinted auricular samples, n = 4.

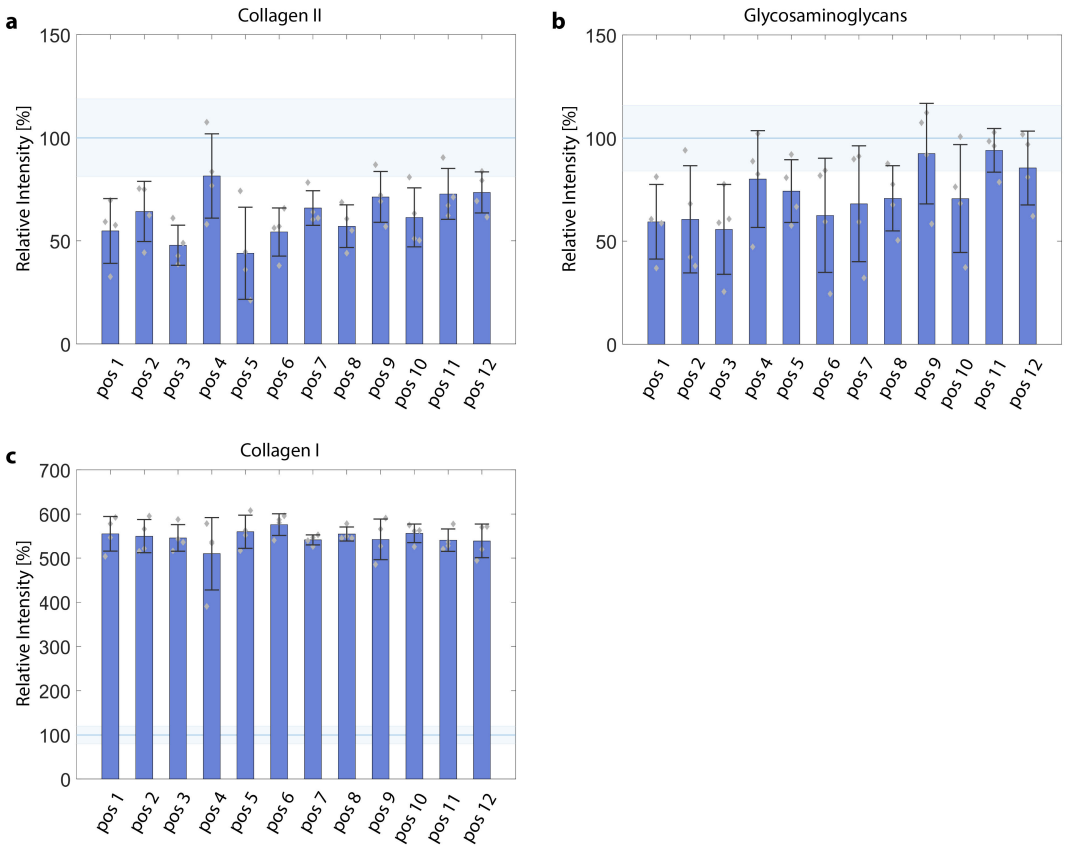

Figure S13. Semi-quantitative analysis of histological and immunohistological stainings of the bioprinted ear. The intensity of histological and immunohistological stainings for a) collagen I, b) GAGs (Safranin O) and c) collagen I were compared to human auricular cartilage (light blue shaded error bar line). n = 4.

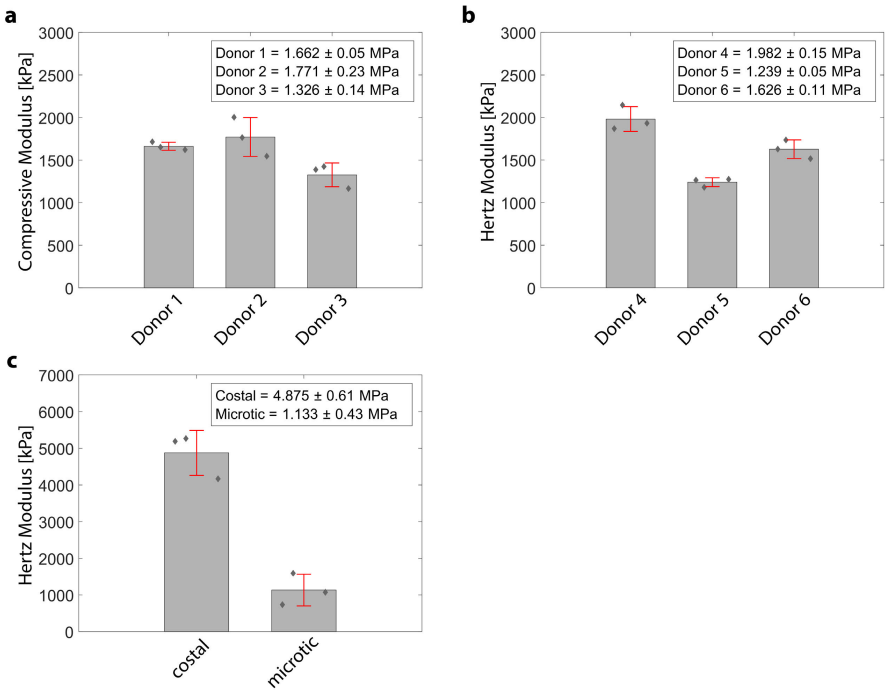

Figure S14. Mechanical analysis of human auricular cartilage as well as coastal and microtic cartilage. a) Compressive modulus of human auricular cartilage of 3 different donors, n = 3. b) Hertz modulus of human auricular cartilage of 3 different donors, n = 3. c) Hertz modulus of human costal cartilage and human microtic cartilage of one donor each, n = 3.

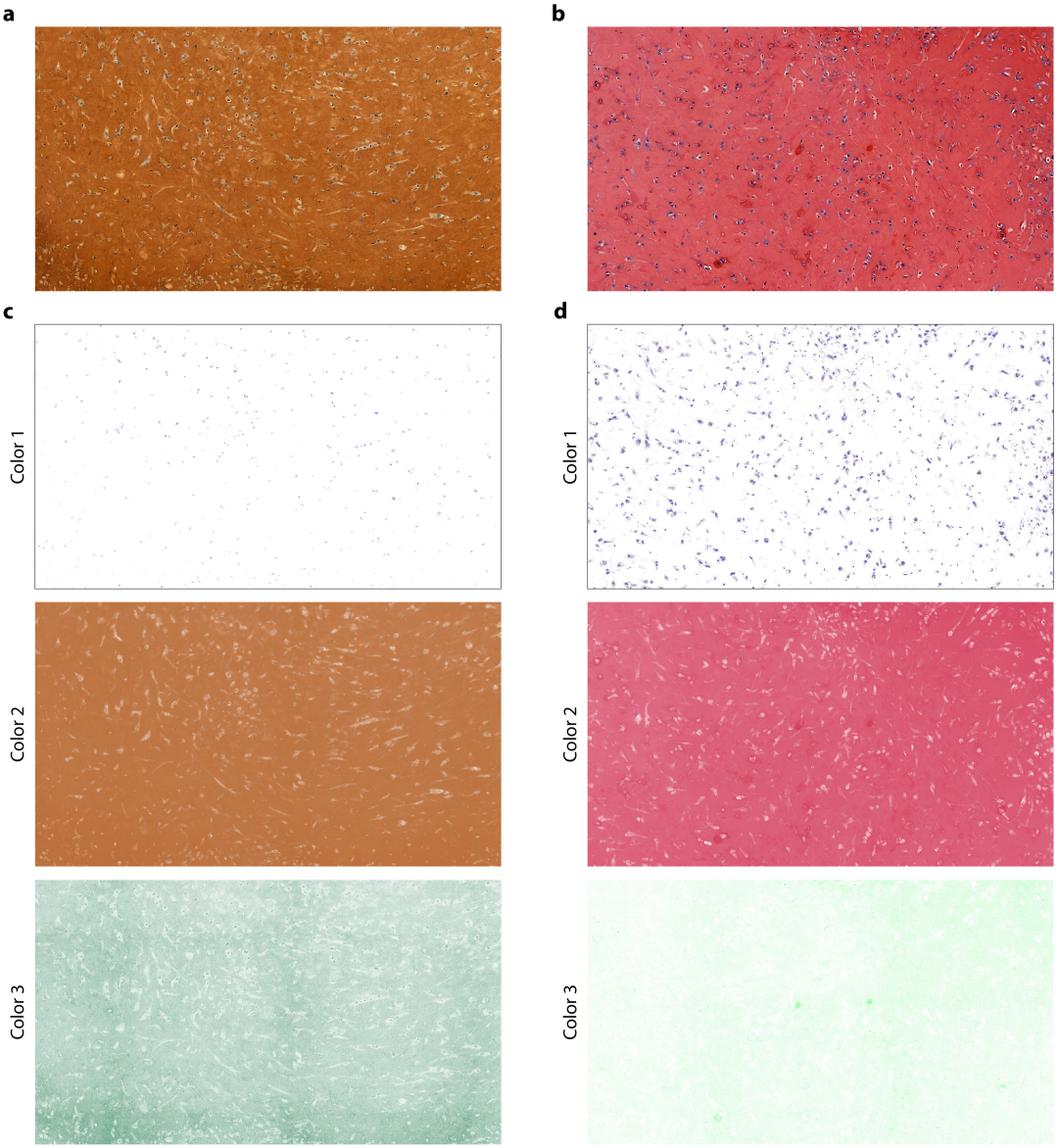

Figure S15. Semi-quantitative analysis of histological and immunohistological images. Sample images of a) immunohistological staining of collagen II and b) Safranin O staining of GAGs of casted sNAG bioink constructs after 9 weeks. c) and d) Color deconvolution of the histological and immunohistological images of a) and b) respectively. Color 1 representing nuclei stained by hematoxylin, color 2 represents matrix components either stained by DAB (collagen I and II, c) or Safranin O (GAGs, d) and color 3 represents an arbitrary color. The mean grey value was then measured in the images depicted in color 2.

Table S1. Shear thinning behavior. Analysis of the shear thinning behavior of the different materials and their combination as well as of the final two bioinks (sNAG bioink and CNF bioink). Viscosity values at shear rates of 0.01 s^{-1} and 300 s^{-1} as well as shear stress values at a shear rate of 0.01 s^{-1}.

Condition	$\eta_{0.01}$ [Pa s]	η_{300} [Pa s]	$\tau_{0.01}$ [Pa s]
1.0% HA	19.7 ± 3.3	0.35 ± 0.01	0.2 ± 0.03
1.5% HA	105.3 ± 6.2	0.87 ± 0.03	1.1 ± 0.06
2.0% HA	292.0 ± 42.5	1.56 ± 0.11	2.9 ± 0.43
1.0% sNAG	94.5 ± 25.3	0.01 ± 0.00	1.0 ± 0.25
2.0% sNAG	686.7 ± 13.6	0.04 ± 0.00	6.9 ± 0.14
3.0% sNAG	1483.3 ± 317.2	0.12 ± 0.00	14.9 ± 3.13
1.0% CNF	261.3 ± 38.2	0.02 ± 0.01	2.6 ± 0.38
2.0% CNF	927.0 ± 324.9	0.26 ± 0.05	9.3 ± 3.24
3.0% CNF	8163.3 ± 2222.2	0.85 ± 0.13	81.7 ± 22.20
1.0% HA + 2.0% sNAG	1646.7 ± 152.8	0.51 ± 0.01	16.5 ± 1.53
1.5% HA + 2.0% sNAG	2056.7 ± 35.12	0.85 ± 0.02	20.6 ± 0.30
2.0% HA + 2.0% sNAG	2666.7 ± 66.6	1.32 ± 0.03	26.7 ± 0.70
0.5% HA + 2.0% CNF	1489.3 ± 498.7	0.34 ± 0.02	14.9 ± 4.99
1.0% HA + 2.0% CNF	1663.3 ± 15.3	0.69 ± 0.00	16.6 ± 0.15
1.5% HA + 2.0% CNF	2090.0 ± 177.8	1.09 ± 0.02	20.9 ± 1.78
sNAG Bioink	1980.0 ± 88.9	1.48 ± 0.02	19.8 ± 0.89
CNF Bioink	1696.7 ± 55.1	1.47 ± 0.02	17.0 ± 0.52

Table S2. Shear recovery behavior. Analysis of the shear recovery behavior of the different materials and their combination as well as of the final two bioinks (sNAG bioink and CNF bioink). Data were analyzed for the recovery of *G'* after the first shear event (G'_{1st}-Recovery) and after the second shear event (G'_{2nd}-Recovery).

Condition	G'_{1st}-Recovery [%]	G'_{2nd}-Recovery [%]
1.0% HA	99.1 ± 0.6	98.8 ± 0.4
1.5% HA	98.8 ± 0.1	98.3 ± 0.1
2.0% HA	98.5 ± 0.6	98.0 ± 1.0
1.0% sNAG	93.4 ± 1.1	90.2 ± 0.4
2.0% sNAG	97.8 ± 8.6	95.5 ± 9.0
3.0% sNAG	88.2 ± 2.5	84.9 ± 1.5
1.0% CNF	51.0 ± 8.5	48.2 ± 8.7
2.0% CNF	42.1 ± 2.0	41.8 ± 2.3
3.0% CNF	74.9 ± 7.3	71.5 ± 6.7
1.0% HA + 2.0% sNAG	82.3 ± 0.3	85.5 ± 0.4
1.5% HA + 2.0% sNAG	106.0 ± 3.3	110.9 ± 3.7
2.0% HA + 2.0% sNAG	125.5 ± 1.2	129.9 ± 0.9
0.5% HA + 2.0% CNF	37.5 ± 1.1	36.8 ± 0.7
1.0% HA + 2.0% CNF	42.3 ± 1.0	42.3 ± 0.9
1.5% HA + 2.0% CNF	63.4 ± 1.6	61.2 ± 1.6
sNAG Bioink	82.8 ± 2.4	84.0 ± 2.4
CNF Bioink	40.7 ± 0.7	38.9 ± 0.6

Table S3. Shear recovery behavior. Analysis of the shear recovery behavior of the different materials and their combination as well as of the final two bioinks (sNAG bioink and CNF bioink). Data were analyzed for *G'* before the first shear event ($G'_{initial}$), after the first shear event (G'_{1st}) and after the second shear event (G'_{2nd}).

Condition	$G'_{initial}$ [Pa]	G'_{1st} [Pa]	G'_{2nd} [Pa]
1.0% HA	25.0 ± 0.1	24.8 ± 0.2	24.7 ± 0.2
1.5% HA	92.6 ± 2.6	91.5 ± 2.5	91.0 ± 2.5
2.0% HA	211.3 ± 36.5	208.3 ± 36.8	207.3 ± 37.1
1.0% sNAG	29.7 ± 0.9	27.7 ± 0.8	26.8 ± 0.7
2.0% sNAG	111.7 ± 5.5	109.0 ± 6.2	106.3 ± 6.8
3.0% sNAG	454.3 ± 10.8	401.0 ± 18.7	385.7 ± 14.5
1.0% CNF	25.1 ± 3.7	12.6 ± 1.0	11. ± 1.2
2.0% CNF	690.7 ± 59.3	291.3 ± 38.8	289.7 ± 41.0
3.0% CNF	2963.3 ± 430.2	2200.0 ± 130.8	2100.0 ± 121.7
1.0% HA + 2.0% sNAG	362.0 ± 16.1	298.0 ± 14.4	309.3 ± 13.2
1.5% HA + 2.0% sNAG	413.3 ± 8.1	438.3 ± 21.4	458.7 ± 23.9
2.0% HA + 2.0% sNAG	556.7 ± 8.5	698.7 ± 16.0	723.0 ± 15.7
0.5% HA + 2.0% CNF	854.7 ± 39.6	320.7 ± 20.5	314.3 ± 14.0
1.0% HA + 2.0% CNF	917.3 ± 57.7	388.7 ± 33.3	388.0 ± 31.7
1.5% HA + 2.0% CNF	866.3 ± 77.4	549.7 ± 58.1	530.7 ± 60.6
sNAG Bioink	496.0 ± 13.9	410.7 ± 22.7	417.0 ± 23.1
CNF Bioink	1000.0 ± 78.4	407.0 ± 36.5	389.3 ± 35.2